20th Australasian Fluid Mechanics Conference
Perth, Australia
5-8 December 2016

Turbulent Pulsatile Pipe Flow with Multiple Modes of Oscillation

W. X. Chen, C. Chin, N. Hutchins, E. K. W. Poon and A. Ooi

Department of Mechanical Engineering
The University of Melbourne, Victoria, 3010 Australia

Abstract

This study numerically investigates turbulent pipe flow driven by a pulsating pressure gradient. While studies of laminar and turbulent pulsatile pipe flow with a single mode of oscillating pressure gradient have been carried out extensively, there is scarce literature on pulsating pressure gradients with multiple temporal Fourier modes. In many real-life engineering applications, for example, the arterial systems, multiple Fourier modes are often required for an accurate representation of the driving force. In this paper, direct numerical simulations are carried out to simulate turbulent pulsatile pipe flow driven by a pressure gradient with 2 Fourier oscillating modes whose mean and extrema are similar to those with a single Fourier mode. The presence of the additional mode of oscillation results in no alterations of the global-mean turbulence statistics such that the mean velocity profiles and turbulence intensities, both collapsing onto its single-mode counterpart. It extends the global-mean characteristics of pulsatile flow from single mode to multiple modes of oscillation. The introduction of an extra Fourier mode in this study diminishes the oscillatory part of the flow such that streamwise velocity modulation amplitudes and the turbulence intensity modulations are reduced. Nevertheless, the present result shows the specific response of an additional Fourier model to the pulsatile turbulence flow analyses. Further investigations are needed to provide a general conclusion on the effect of other additional Fourier modes.

Introduction

Pulsatile flow in a rigid pipe represents a fundamental model for a wide range of practical engineering problems, from blood flow in arteries to internal combustion engines. The term *pulsation* refers to flow driven by the pressure gradient by superimposing unsteady forcing terms to a steady component, opposite to *oscillation* where flow is only driven by the oscillatory component with a zero mean. Laminar pulsatile flow is well understood with the work by Womersley [11] and Uchida [10] in the 1950's. The so-called Womersley profile characterises velocity profiles of laminar pulsatile pipe flow. However, chaotic and turbulent pulsatile flow exits due to the comlex interactions between the forcing oscillation and the steady part of the flow. For example, blood flow in human aorta is one type of high-frequency turbulent pulsatile flow which could reach a maximum bulk Reynolds number $Re_b \approx 6500$ ($Re_b = U_b D/\nu$ where U_b is the bulk velocity and ν is the kinematic viscosity) [4].

Turbulent pulsatile pipe flow has often been studied with the assumption of oscillating pressure gradient with a single Fourier mode. This simplification treats the pressure gradient as one sinusoidal component superimposed onto a steady component. Another two dimensionless parameters besides the bulk Reynolds number Re_b were introduced: the oscillatory Reynolds number $Re_\omega = U_m^2/\omega\nu$ (where U_m is the maximum value of the oscillatory flow at the centre of the pipe and ω is the oscillation frequency) and the ratio of the oscillating velocity to the mean bulk velocity $\beta = U_m/U_b$. Lodahl et al. [3] conducted a series of experimental studies covering a wide range of Reynolds numbers, oscillation amplitudes and frequencies. The flow was classified *current-dominated* if $\beta \leq 1$, or otherwise *wave-dominated*. They identified regions of laminar and turbulent flow based on the oscillation amplitudes and frequencies. They also showed the critical values of these parameters that result in flow relaminarisation. Direct numerical simulations at the identical $Re_b \approx 5900$ by Manna et al. [4] demonstrated that the existing turbulence due to the steady component was not affected by the additional unsteady forcing term provided that the resulting flow was in the current-dominated regime. In contrast, turbulent statistics were altered when the flow was in the wave-dominated regime and drag reduction was achieved as a result of a thickened viscous sublayer. The effect of pulsations is also determined by the frequency of the imposed modulation. Pulsation at relatively low frequency where the turbulent Stokes number $\Omega_t < 10$ ($\Omega_t = \omega D/u_\tau$) does not modify the turbulence structure and the production of turbulence is still governed by the turbulent bursting frequency f_{burst}. When $\Omega_t > 10$ in which oscillations are considered to be in the high frequency regime, near-wall turbulence production interacts with the imposed oscillation but the bulk flow at the centre of the pipe exhibits a solid-body-like oscillation [7].

The flow behaviours in human aorta or in engines, however, are rather complex and could not be represented by a single sinusoidal term. These aforementioned literature studying pulsatile flow with a single mode of oscillating pressure gradient may not provide accurate estimations of pulsatile flow behaviours in the turbulent regime. In the present study, an additional term was introduced to the pressure gradient such that it could no longer be represented by a single sinusoidal frequency. The increasing number of Fourier modes is expected to add complexity but to provide advanced information about real-life modulations of pulsatile flow. Our numerical solver and grid resolution were validated by comparing to published results of Manna et al. [4]. The extra mode of oscillation was then introduced such that the mean and the extrema of the pressure gradient were nearly identical to those used in the single mode of oscillation. The global-mean turbulence statistics including the velocity profile and turbulence intensities from both single-mode and multi-mode studies were analysed and compared. The effects of the additional mode on the modulations of statistics were addressed by decoupling the oscillatory flow component from the steady part.

Methodology

Direct numerical simulations were performed with incompressible Newtonian fluids. The governing equations are the incompressible Navier–Stokes equations with a pressure gradient (source term),

$$\frac{\partial \mathbf{u}}{\partial t} + \mathbf{u}\cdot\nabla\mathbf{u} - \nu\nabla^2\mathbf{u} + F = -\frac{1}{\rho}\nabla p, \tag{1}$$

$$\nabla\cdot\mathbf{u} = 0, \tag{2}$$

where ρ is density; p is the pressure; F is the total pressure gradient in the streamwise z direction and $\mathbf{u} = (u_x, u_y, u_z)$. For convenience, we coverted Cartesian to polar coordinates in our analysis such that $\mathbf{u} = (u_r, u_\theta, u)$ representing the velocity in the

radial, azimuthal and streamwise directions respectively. The total pressure gradient comprises the mean and the oscillatory components,

$$F = F_0 + \sum_{n=1}^{\infty} F_{cn,n}\cos(n\omega t) + F_{sn,n}\sin(n\omega t), \tag{3}$$

where n represents the n^{th} mode of oscillation in the Fourier series, $F_{cn,n}$ and $F_{sn,n}$ are the amplitudes of modulation of the n^{th} mode.

The simulation parameters of our validation cases in the current-dominated regime (referred as SSCD namely **S**ingle-mode **S**ingle-term **C**urrent **D**ominated case) and in the wave-dominated regime (**S**ingle-mode **S**ingle-term **C**urrent **D**ominated case, SSWD) were selected to match those in [4]. A single oscillating pressure gradient term of the 1st Fourier mode was applied such that the resultant pressure gradient was

$$F_{ss} = F_0 + F_{cn,1}\cos(\omega t). \tag{4}$$

where the subscript v represents the cases of validation.

Another analysis was performed by sequentially adding the sine term from the first Fourier mode (referred as **S**ingle-mode **M**ulti-term **C**urrent **D**ominated case, SMCD),

$$F_{sm} = F_0 + F_{cn,1}\cos(\omega t) + F_{sn,1}\sin(\omega t). \tag{5}$$

and a cosine term from the second Fourier mode (**M**ulti-mode **M**ulti-term **C**urrent **D**ominated case, MMCD),

$$F_{mm} = F_0 + F_{cn,1}\cos(\omega t) + F_{sn,1}\sin(\omega t) + F_{cn,2}\cos(2\omega t). \tag{6}$$

The time-dependent pressure gradient waveforms for the current-dominated cases are plotted in figure 1. The mean and the extrema of pressure gradients in SMCD and MMCD are maintained similar for investigations.

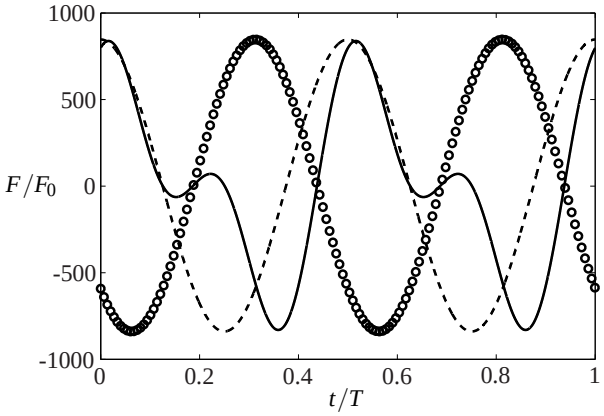

Figure 1. Forcing terms (pressure gradients) for −− SSCD (single-mode single-term); ◦ SMCD (single-mode multi-term); — MMCD (multi-mode multi-term).

The system of governing equations (1) and (2) was solved using a finite volume method, OpenFOAM 2.1.1 (OpenCFD, Ltd., ESI group, Bracknell, UK) C++ library. The Pressure Implicit with Splitting of Operator (PSIO) method was employed for the velocity-pressure coupling. Periodic boundary conditions were applied in the streamwise direction. The boundary conditions were no-slip for velocity and Neumann for the pressure at the wall. A pipe of diameter $D = 1$ and a length of $2\pi D$ was used. An O-grid was used with grid resolutions in terms of wall units based on the mean u_τ of each validation case as tabulated in table 1.

Turbulence statistics were collected after 100 cycles of pulsation. Statistics were calculated over the next 5 cycles based on 32 evenly spaced time points per cycle. Following the triple decompositions in [9], any quantity φ can be decoupled in terms of the steady and oscillatory parts,

$$\varphi = \langle\varphi\rangle + \varphi' = \overline{\langle\varphi\rangle} + \widetilde{\varphi} + \varphi', \tag{7}$$

where $\langle\varphi\rangle$, $\overline{\langle\varphi\rangle}$, and φ' are the phase-mean, the global-mean, and the turbulence fluctuation of φ respectively. $\widetilde{\varphi}$ represents the modulation of quantity φ against the global-mean value due to the imposed pulsation, which can be computed as,

$$\widetilde{\varphi} = \sum_{n=1}^{\infty} \widehat{\varphi}_n \cos(n\omega t + \phi_n), \tag{8}$$

where $\widehat{\varphi}_n$ is the amplitude of oscillation and ϕ_n is the phase of the n^{th} mode.

The analytical solution derived by Womersley [11] governs the laminar oscillatory flow,

$$\tilde{u} = \mathrm{Re}\left[\frac{-i\widehat{F_{mod}}}{\omega}\frac{1 - J_0\left(i^{\frac{3}{2}}\sqrt{\frac{\omega}{\nu}}\right)}{J_0\left(i^{\frac{3}{2}}R\sqrt{\frac{\omega}{\nu}}\right)}\exp(i\omega t)\right], \tag{9}$$

where $\tilde{u}$ represents the modulation of the streamwise velocity and $\widehat{F_{mod}}$ is the amplitude of the oscillating forcing component (pressure gradient).

	Re_τ	z^+	x^+_{max}	y^+_w
SMCD	200	6.4	2.06	0.067
SMWD	160	2.9	1.66	0.041

Table 1. Computational grid resolution.

Numerical Validations

A validation simulation was first conducted to test the capability of the OpenFOAM solver to accurately simulate pulsatile flow in the turbulent regime. To the authors' knowledge, similar solvers have been tested by Papadopoulos and Vouros [6] but only when the flow is within the current-dominated regime. It is an essential step to confirm the adequate grid type and resolution for pulsatile flow in the wave-dominated regime because of excessive modulation amplitudes. As the settings of our simulation were similar to cases by Manna et al., the mean velocity profiles and turbulence intensities were compared against the DNS results in [4]. The flow statistics in both current- and wave-dominated regimes agree well with those by Manna et al. [4] but only the streamwise mean velocity profiles are plotted here.

Figure 2 shows the mean velocity profiles of the present validation simulations compared to those from literature [4, 1]. The mean velocity profile of SSCD case collapses onto its steady counterpart profile. This shows that the turbulence in the current-dominated regime is not affected by the imposed oscillating pressure gradients in the spatio-temporal manner. On the other hand, the velocity profile of SSWD case is in a reasonably good agreement with the wave-dominated data in [4]. The buffer layer of the mean velocity is lifted up compared to the steady case, leading to a higher viscous scaled velocity towards the centreline. This implies a reduction of skin friction with respect to the steady case, which is reflected by the decrease of global Re_τ in table 1.

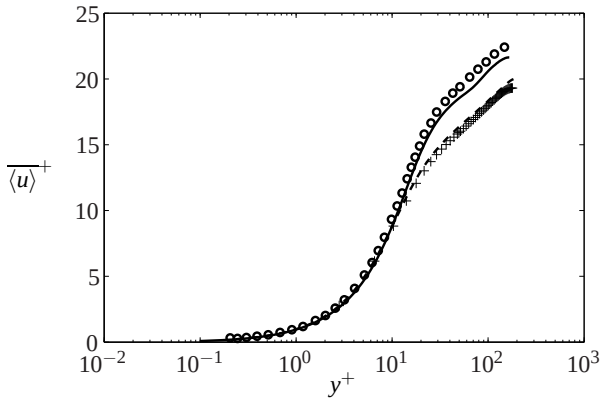

Figure 2. Mean velocity profiles. −− SSCD (single-mode single-term current-dominated); — SSWD (single-mode single-term wave-dominated); ∘ wave-dominated data of Manna et al. [4]; + steady pipe data of Eggels et al. [1].

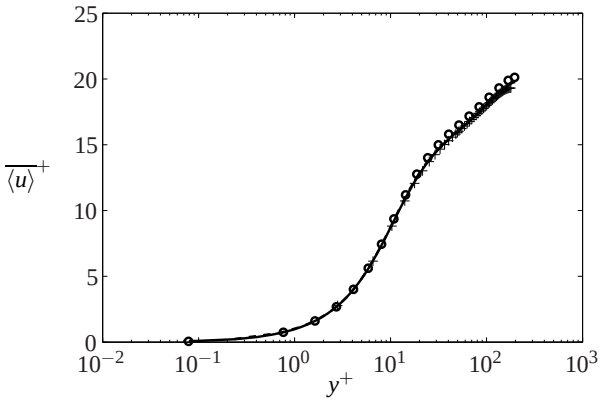

Figure 3. Global-mean velocity profiles. −− SSCD (single-mode single-term); ∘ SMCD (single-mode multi-term); — MMCD (multi-mode multi-term); + steady pipe data of Eggels et al. [1].

Flow with Multiple Oscillating Modes

Global-Mean Statistics

Table 2 summarises the global-mean flow properties of simulated cases SSCD, SMCD and MMCD. As both mean and the extrema of the pressure gradients were almost identical (see figure 1), the global-mean flow statistics (e.g. friction u_τ, bulk U_b and centreline U_c velocities) for all cases are quantitatively similar, indicating the resultant flow is within the same flow regime. On the other hand, both SSCD and SMCD have nearly identical U_m/U_b ratio (β) and oscillatory Reynolds number Re_ω; but U_m and consequently Re_ω decrease for MMCD. This implies a weakening effect on the oscillatory flow component when the 2nd mode of oscillation in this study is present. Our present result demonstrates a non-linear relationship between the forcing term F and U_m under the effect of additional mode of oscillation. This non-linear correlation cannot be predicted using the laminar Womersley solution in equation (9) any more.

	SSCD	SMCD	MMCD
U_b/u_τ	15.39	15.43	15.16
U_c/u_τ	20.12	20.12	19.76
U_c/U_b	1.30	1.30	1.31
$Um/U_b(\beta)$	0.98	0.99	0.89
Re_τ	198	196	199
Re_b	6068	6057	6042
Re_ω	1600	1607	1295

Table 2. Mean flow properties comparison.

Figure 3 shows the global-mean, radial distribution of the streamwise velocity in inner coordinates. Global-mean velocity profiles for all case (SSCD, SMCD and MMCD) collapse on the classic turbulent pipe flow velocity profile with steady driving force at equivalent Re_τ. It implies the additional 2nd Fourier mode of oscillation has insignificant effect on the global-mean velocities. The rms values of u', u'_r, u'_θ fluctuating about the phase-mean values are shown in figure 4. All rms profiles are consistent to each other. As a result, in the current-dominated flow regime, the global-mean turbulence statistics are not affected by the imposed oscillations regardless of the number of oscillating modes, further extending the characteristics of pulsatile flow to multi-mode oscillations from the literature [3, 4, 7, 8, 9].

Phase-mean Statistics

Figure 5 depicts the time variation of $\widetilde{rms(u')}^+$ of SSCD and

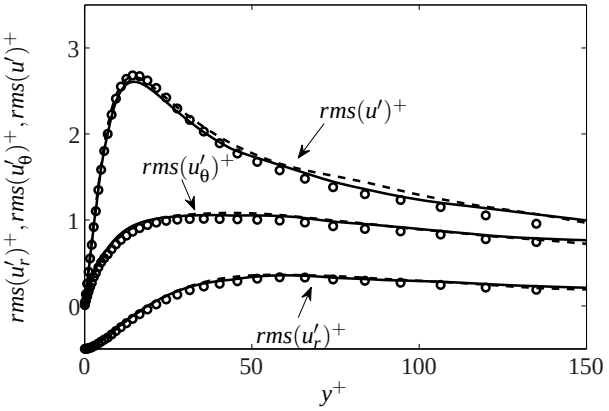

Figure 4. Global-mean turbulence intensities. −− SSCD (single-mode single-term); ∘ SMCD (single-mode multi-term); — MMCD (multi-mode multi-term).

MMCD in inner coordinates for one period of oscillation (results from SMCD are not shown as they are shifted in phase by $\pi/4$ to SSCD case). The modulation term describing the effect due to the imposed oscillation against the global-mean values is obtained based on equations (7) and (8). In both cases the modulations can be treated as a wave that is initiated at the wall (identified by a change from negative to positive gradient near the wall, see figure 5 at $3pi/4$), propagating towards the centreline and eventually diffuses at $y^+ \sim 40$. These are consistent with the description in Manna et al. [5]. In SSCD, the change in gradients occurs between $\pi/2$ and $3\pi/4$ implying a formation of wave in-between these two phases. On the other hand, the initiation of the wave for MMCD lies between $3\pi/4$ and π, indicating a lag $\sim \pi/4$ compared to SSCD. This phase lag continues throughout the life cycle of the wave. In addition, the MMCD case is governed by a lower turbulence intensity modulation compared to the SSCD case. It is consistent with the weakened oscillatory component of the flow in MMCD indicated by the decrease of Re_ω in table 2.

Figure 6 illustrates the modulations of the streamwise velocity. The maxima in MMCD is significantly less than those in SSCD and SMCD due to the presence of the additional mode. The decreasing amplitude in the streamwise velocity modulation may be depending on the phase of the 2nd mode. An additional 2nd Fourier mode in-phase with the primary mode is expected to enhance the oscillatory flow and consequently, the fluctuations of turbulence against the global mean value. It requires further

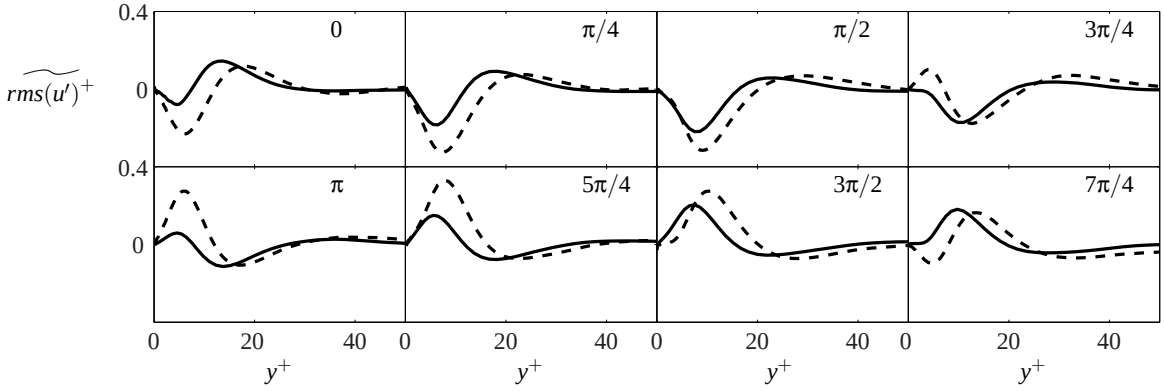

Figure 5. Temporal variation of the streamwise turbulence intensity modulation against global-mean values. −− SSCD case;— MMCD case.

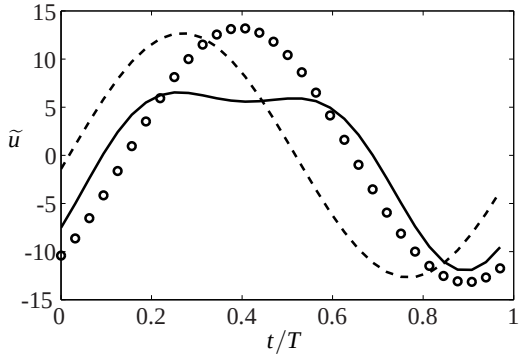

Figure 6. Streamwise velocity modulations against global-mean values. −− SSCD (single-mode single-term); ∘ SMCD (single-mode multi-term); — MMCD (multi-mode multi-term).

studies to provide a conclusion about authors' speculations.

Conclusions

Pulsatile pipe flow driven by multiple Fourier modes of oscillating pressure gradients was studied with direct numerical simulations in the current-dominated regime and was compared to its counterparts with single mode of oscillation. The numerical results confirmed the capability of our computational methodology and grid resolution for simulations on pulsatile pipe flow in both current- and wave-dominated regimes by validating the turbulence statistics against those reported in the literature. Pulsatile pipe flow with multiple modes of oscillation was shown to follow the characteristics of that with single mode by examining the global-mean velocities and turbulence intensities. However, it was shown that modulations of the flow quantities against their global-mean values including streamwise velocity and turbulence intensity were affected by the additional Fourier mode. Although the oscillating effect of the flow was diminished by our choice of the 2nd Fourier mode, there might be cases where the inverse effect could be gained as the overall waveform of the forcing term may depend on the phase of the additional oscillating mode relative to the primary terms.

Acknowledgements

This work was supported by the ARC Linkage Project (LP150100233) and VLSCI high performance computing grant (VR0210).

References

[1] Eggels, J.G.M., Unger, F., Weiss, M.H., Westerwell, J., Adrian, R.J., Friedrich, R. and Nieuwstadt, F.T.M., Fully Developed Turbulent Pipe Flow: A Comparison between Direct Numerical Simulation and Experiment, *Journal of Fluid Mechanics*, **268**, 1994, 175–210.

[2] Erbel, R. and Eggebrecht, H., Aortic Dimensions and the Risk of Dissection, *Heart* , **92**, 2006, 137–142.

[3] Lodahl, C.R., Sumer, B.M. and Fredsoe, J., Turbulent Combined Oscillatory Flow and Current in a Pipe, *Journal of Applied Physiology*, **20**, 1998, 1078–1082.

[4] Manna, M., Vacca, A. and Verzicco, R., Pulsating Pipe Flow with Large-amplitude Oscillations in the Very High Frequency Regime. Part 1. Time-averaged Analysis, *Journal of Fluid Mechanics* , **700**, 2012, 246–282.

[5] Manna, M., Vacca, A. and Verzicco, R., Pulsating Pipe Flow with Large-amplitude Oscillations in the Very High Frequency Regime. Part 1. Phase-averaged Analysis, *Journal of Fluid Mechanics* , **766**, 2015, 272–296.

[6] Papadopoulos, P.K. and Vouros, A.P., Pulsating Turbulent Pipe Flow in the Current Dominated Regime at High and Very-high Frequencies, *International Journal of Heat and Fluid Flow* , **58**, 2016, 54–67.

[7] Ramaprian, B.R. and Tu, S.W., Fully Developed Periodic Turbulent Pipe Flow. Part 2. The Detailed Structure of the Flow, *Journal of Fluid Mechanics* , **137**, 1983, 59–81.

[8] Scotti, A. and Piomelli, U., Numerical Simulation of Pulsating Turbulent Channel Flow, *Physics of Fluids* , 13 , 2001, 1367-1384.

[9] Tardu, S.F., Binder, G. and Blackwelder, R.F., Turbulent Channel Flow with Large-amplitude Velocity Oscillations, *Journal of Fluid Mechanics* , **267**, 1994, 109-151.

[10] Uchida, S., The Pulsating Viscous Flow Superposed on the Steady Laminar Motion of Incompressible Fluid in a Circular Pipe, *Zeitschrift fr angewandte Mathematik und Physik ZAMP*, **7**, 1956, 403–422.

[11] Womersley, J.R., Method for the Calculation of Velocity, Rate of Flow and Viscous Drag in Arteries when the Pressure Gradient is Known, *The Journal of Physiology*, **127**, 1955, 553–563.